MVA2007 IAPR Conference on Machine Vision Applications, May 16-18, 2007, Tokyo, JAPAN

Detection of Fundus Lesions using Classifier Selection

Hiroto Nagayoshi
Yoshitaka Hiramatsu
Hiroshi Sako

Central Research Laboratory,
Hitachi Ltd., Tokyo, Japan

{ hiroto.nagayoshi.wy,
yoshitaka.hiramatsu.xw,
hiroshi.sako.ug }@hitachi.com

Mitsutoshi Himaga

Hitachi-Omron Terminal
Solutions, Corp., Aichi, Japan

mitsutoshi_himaga@
hitatchi-omron-ts.com

Satoshi Kato

Department of Ophthalmology,
The University of Tokyo,
School of Medicine,
Tokyo, Japan

katou-s@ka2.so-net.ne.jp

Abstract

A system for detecting fundus lesions caused by diabetic retinopathy from fundus images is being developed. The system can screen the images in advance in order to reduce the inspection workload on doctors. One of the difficulties that must be addressed in completing this system is how to remove false positives (which tend to arise nearby blood vessels) without decreasing the detection rate of lesions in other areas. To overcome this difficulty, we developed so-called "dynamic selection" of a classifier according to the position of a candidate lesion, and we introduced new features that can distinguish true lesions from false positives. The system—incorporating dynamic selection and these new features—was tested in experiments using 55 fundus images with some lesions and 223 images without lesions. The results of the experiments confirm the effectiveness of the proposed system, namely, degrees of sensitivity and specificity of 98% and 81%, respectively.

1 Introduction

Though efforts to prevent diabetic retinopathy have been ongoing for more than 20 years, diabetes has been still one of the most serious diseases in many countries. Patients are always threatened by the fear of blindness caused by diabetic retinopathy [1]. In Japan, the number of people who take medical examinations in order to keep their health in good condition has been increasing. During the examination of diabetic retinopathy, the doctor examines fundus images taken by special cameras. However, the current situation that the number of images is increasing drastically makes the doctor's workload very heavy. This is the reason that a CAD (computer aided detection) system for automatically detecting diabetic retinopathy is eagerly expected.

Usher et al. developed a system to detect the lesions of diabetic retinopathy [2][3]. The system is comprised of image normalization (step 1), image analysis for detecting basic portions such as the blood vessels and the optic disk (step 2), detection of candidate lesions (step 3), and discrimination of true lesions from false positives (FPs) (step 4). Here, FPs are not lesions but portions detected as lesions incorrectly. Step 2 excludes the portions of blood vessels and the optic disk from the whole fundus image, because these portions usually have no diabetic retinopathy lesions and the color of the portions is very similar to that of lesions. This step can simplify the discrimination of true lesions (TLs) from false positives (FPs) in the next step. The detection of candidate lesions is executed by a special segmentation based on region growing and adaptive binarization. Step 4 uses a neural network that utilizes the intensity and geometrical features detected from the candidate lesions.

In Usher's system, the positions of candidate lesions are not utilized in the classifier. But our research revealed that the FPs tend to arise in nearby blood vessels, because the intensity around the blood vessels varies complicatedly and the classification is very difficult. This fact will contribute to decreasing the number of FPs.

This paper firstly describes the intensity normalization essential for precise detection of lesions and the detection of basic portions as preprocesses. Secondly, it is shown that the degree of difficulty in lesion detection varies with the distance between a lesion and its nearest blood vessel. This fact leads to the idea of "classifier selection" for decreasing the number of FPs around blood vessels. Thirdly, actual classification based on some new features from the periphery of candidate lesions is proposed. Finally, a system applying the proposed techniques is evaluated by experiments using actual fundus images.

2 Detection of lesions

Fig. 1 shows the flow diagram of the lesion detection process. The left and the right sides of the figure indicate

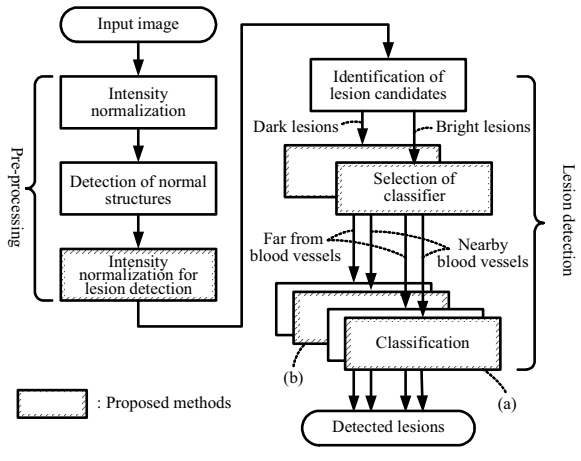

Figure 1. Flow of lesion detection

the pre-processing parts and the lesion detection parts, respectively. In this process, intensity normalization and classifier selection are introduced, and new features that allow the classifier to detect candidate lesions around blood vessels are also introduced.

2.1 Detection of basic portions

The detection of basic portions such as blood vessels and the optic disk from an input image is done by pre-processing. The intensity of the input image is normalized in advance using Sinthanayothin's method [4].

Himaga's method [6] can be used to extract blood vessels. With this method, first, the input image is transformed into an image in which the blood vessel regions are emphasized by matched filters composed of Gaussian kernels. Directional recursive region growing segmentation (D-RRGS) technique is then applied to the image to extract blood vessel regions. The extraction of the optic disk can be completed by the matching with a standard template of an average image of the optic disk patterns.

2.2 Intensity normalization for lesion detection

Intensity normalization is necessary for detecting true lesions because their intensities are essential features. This normalization consists of two processes: area-dependent normalization (ADN) and area-independent normalization (AIN). The objective of the ADN is to correct the low brightness of the pixels at the outskirts of a fundus image caused by the lack of lighting intensity and the aberration of the lenses, while the objective of AIN is to remove the difference in the intensity of the individual fundus and that of the lighting environment.

In ADN, first, a window around a target pixel r_0 to be normalized is set. And $R_W(r_0)$ is denoted as the pixel set in the window and R_F as the pixel set of the whole fundus image except the blood vessels and the optic disk. The difference of ADN from Sinthanayothin's method [4] is that the average and standard deviation that are used to correct V (in an HSV color system) at r_0 are calculated in region $R_W(r_0) \cap R_F$, because the existence of the blood vessels in $R_W(r_0)$ affects them.

The equations used in ADN are shown from (1) to (3).

$$\tilde{v}(r_0) = \{v(r_0) - avg(v(r), r_0)\} / stdev(v(r), r_0) \quad (1)$$

$$avg(v(r), r_0) = \frac{1}{|R_W(r_0) \cap R_F|} \sum_{r \subset R_W(r_0) \cap R_F} v(r) \quad (2)$$

$$stdev(v(r), r_0) = \sqrt{\frac{1}{|R_W(r_0) \cap R_F|} \sum_{r \subset R_W(r_0) \cap R_F} \{v(r) - avg(v(r), r_0)\}^2} \quad (3)$$

$v(r)$: V at r before normalization
$\tilde{v}(r)$: V at r after ADN
$avg(v(r), r_0)$: average of V in $R_W(r_0) \cap R_F$
$stdev(v(r), r_0)$: standard deviation of V in $R_W(r_0) \cap R_F$
$|R|$: the number of elements in set R

After ADN, AIN is applied to the whole fundus image except the blood vessels and the optic disk for correcting the difference in the intensity of the individual fundus and that of the lighting environment. AIN uses the average and the standard deviation of V given by equations (4) to (6).

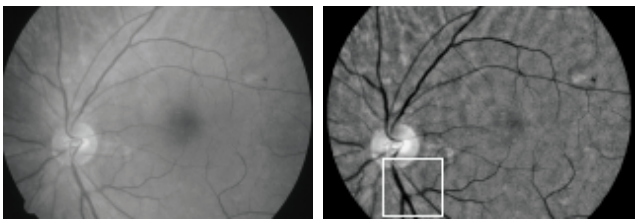

(a) Input image (b) Normalized image
Figure 2. Intensity normalization

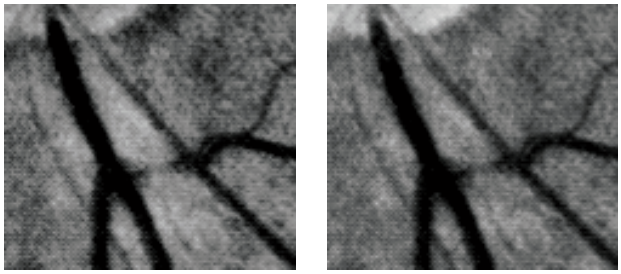

(a) Conventional method (b) Proposed method
Figure 3. Comparison of the intensity normalization methods

$$\hat{v}(r_0) = a_0 \{\tilde{v}(r_0) - avg(\tilde{v}(r))\} / stdev(\tilde{v}(r)) + b_0 \quad (4)$$

$$avg(\tilde{v}(r)) = \frac{1}{|R_F|} \sum_{r \subset R_F} \tilde{v}(r) \quad (5)$$

$$stdev(\tilde{v}(r)) = \sqrt{\frac{1}{|R_F|} \sum_{r \subset R_F} \{\tilde{v}(r) - avg(\tilde{v}(r))\}^2} \quad (6)$$

$\hat{v}(r)$: V at r after AIN
a_0 and b_0: constants
$avg(\tilde{v}(r))$: average of V in R_F
$stdev(\tilde{v}(r))$: standard deviation of V in R_F

An example of the intensity normalization is shown in Fig. 2. In the figure, (a) is the original image and (b) is the normalized image. It can be seen that the shadow at the outskirts of (a) is corrected in (b). Fig. 3 is a magnified image of the white rectangle area in Fig. 2(b). In Fig. 3, (a) is the result of the conventional method in which blood vessels and optic disk are used to calculate $avg(v(r), r_0)$ and $stdev(v(r), r_0)$, and (b) is that of the proposed method. In comparing the intensities of the areas between blood vessels, it is clear that those of Fig. 3(a) are brighter than those of Fig. 3(b). This is because the calculation of $avg(v(r), r_0)$ of equation (1) includes blood vessels whose intensities are low, as in Fig. 3(a). When $avg(v(r), r_0)$ becomes low, according to equation (1), the normalized value $\tilde{v}(r)$ will be high apparently. On the other hand, that kind of problem such a high $\tilde{v}(r)$ does not occur in the case of the proposed method.

2.3 Detection of candidate lesions

The segmentation and the adaptive thresholding technique are utilized to detect candidate lesions [2][3]. They are applied to the G-image in a RGB color system, because the G-image has the most information in fundus images [5][7]. The region growing method is used for this segmentation. This method makes groups from pixels with similar values: that is, it can extract one candidate region (i.e., a set of pixels) as one lesion. Next, adaptive thresholding is applied to the G-image with segmented region

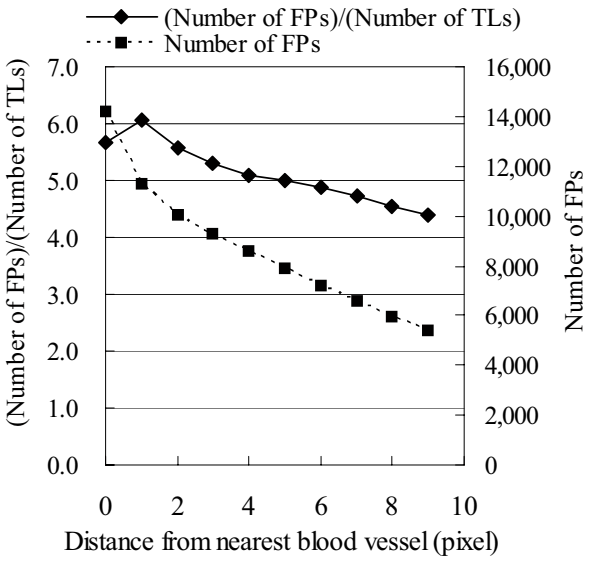

Figure 4. Number of FPs (bright lesions) according to the distance from nearest blood vessel

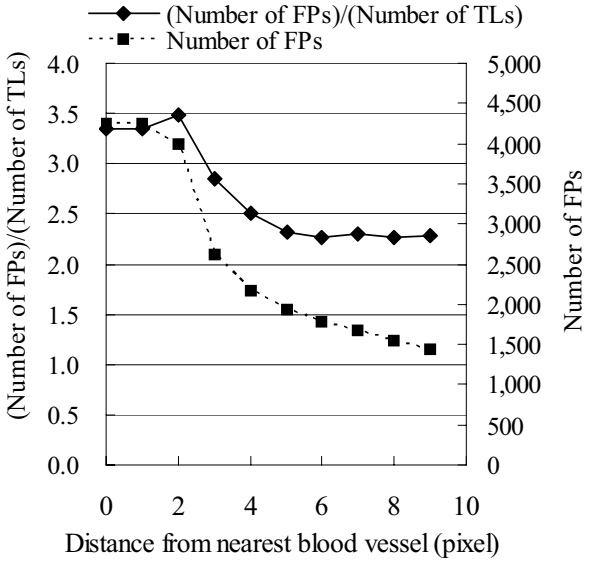

Figure 5. Number of FPs (dark lesions) according to the distance from nearest blood vessel

information. The regions whose average G-value is brighter than the peripheries' G-value are detected as bright lesions. Such regions are exudates and cotton wool spots. The regions whose average value is darker than their peripheries' value are detected as dark lesions such as microaneurysms and haemorrhages.

2.4 Classifier selection

The analysis of detected candidate lesions proved that FPs arise more frequently nearby blood vessels as shown in Figs. 4 and 5. The horizontal axis indicates the city block distance of a FP from its nearest blood vessel. The broken line indicates the number of FPs that are more than the value on the horizontal axis away from their nearest blood vessels. The solid line indicates the ratio of the number of FPs against the number of TPs. According to Figs. 4 and 5, the nearer a candidate lesion is to its nearest blood vessel, the higher probability that the candidate is a FP. To increase the reliability of our system, this fact can be made good use of in our approach to reduce the number of FPs.

The candidate lesions far from their nearest blood vessels can be classified by using neural networks [2][3]. The input features are average intensity, geometric characteristics of the candidate lesion, and so on. On the other hand, the candidate lesions around the blood vessels are classified by a classifier based on rules using several new features. The features include intensity, area, shape of the candidate and relative intensity to its periphery. The latter classifier is described in Section 2.5.

The classifier for a candidate lesion is selected according to its distance from its nearest blood vessel. A different threshold distance for selecting a classifier has been determined for each kind of lesion. Because the slope of a solid line of bright lesions (shown in Fig. 4) is not steep, the one-pixel-distance covering the peak is set as the threshold. Candidate lesions whose distance from their nearest blood vessel is within one pixel are input into the new classifier for bright lesions, while the other candidates are input into the neural networks for bright lesions. On the other hand, the solid line of dark lesions (shown in Fig. 5) is dull more than a distance of four pixels; therefore, four-pixel-distance is set as the threshold. The procedure of this classifier selection is the same as that in the bright lesion case. (Note that above thresholds are determined under the condition that the image size is 700×605 pixels. In the case of a different image size, it is necessary to change the thresholds accordingly.)

2.5 New classifier

As described above, a different classifier is utilized according to the distance from the nearest blood vessel to the candidate lesion. A neural network, which uses features such as intensity and geometric characteristics is applied to classify the candidate lesions far away from the nearest blood vessel [2][3].

To design the new classifier for the candidate lesions around the nearest blood vessels, the following two features must be considered: (i) regions that are bright and lie along the blood vessels tend to be FPs of bright lesions and (ii) partial regions that cannot be extracted as blood vessels tend to be FPs of dark lesions. To discriminate these FPs from true lesions, we proposed the following new features.

2.5.1 Bright lesion

In this subsection, the classifier that corresponds to Fig. 1(a) is explained. Regarding the difference between the features of type-(i) FPs and those of true lesions, it is shown that FP's intensity gives a weak contrast with its periphery and that it has a line-shape along the blood vessel. To obtain the intensity contrast, one new feature is proposed, namely, the ratio of the average of *G* (in a RGB color system) in a candidate lesion (Fig. 6(a)) to the one at the periphery (Fig. 6(d)). Hereafter, we call this feature "G-ratio". The G-ratio near the value of 1 means that the lesion has almost the same intensity as its peripheral. The high G-ratio, much more than 1, means that the lesion is much brighter than its peripheral, and vice versa. On the other hand, to obtain the shape feature of a FP, another new feature is proposed. This feature is based on the de-

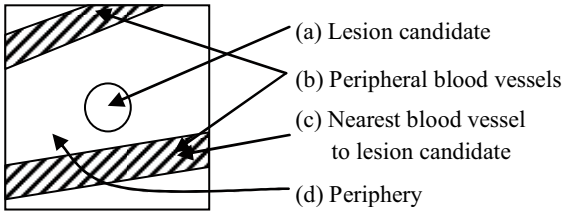

Figure 6. Lesion candidate and nearby blood vessels

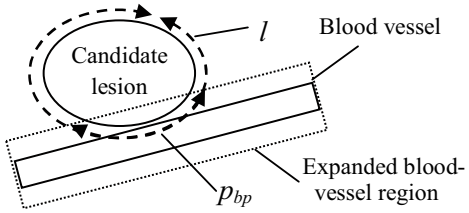

Figure 7. Degree of touching between a lesion candidate and a blood vessel

gree of touching between the candidate lesion and a peripheral blood vessel. Hereafter, we call it "T-degree", which is calculated from equation (7)

$$T_d = p_{bp} / l \tag{7}$$

where l denotes the length of the contour of the candidate lesion, and p_{bp} denotes the number of pixels of its contour that are in the expanded blood vessel region (Fig. 7). When the candidate lesion is thin and close to the blood vessel, T-degree will be high.

The classification for the type-(i) bright lesions uses G-ratio, T-degree, and an additional feature to remove the noise, namely, the area of the candidate lesion. In order to examine the new features' effectiveness, simple classifier is appropriate. Thus, we adopted simple thresholding as a classifier. The threshold for each feature is determined in advance by analyzing distribution of each faeture. The candidate lesion whose features exceed all thresholds is regarded as a true bright lesion in this classification.

2.5.2 Dark lesion

In this subsection, the classifier that corresponds to Fig. 1(b) is explained. Table 1 lists the characteristics of TLs and FPs among dark lesion candidates. Most type-(ii) FPs arise under conditions #2 or #4. Further investigation of the type-(ii) FPs suggests G (in RGB color system) of the type-(ii) FP tends to be brighter than that of the peripheral blood vessels (Fig. 6(b)). Therefore, a new feature, called G-BV-difference, namely, the difference between average G in candidate lesions (Fig. 6(a)) and average G in the peripheral blood vessels (Fig. 6(b)), is assigned.

As described in 2.5.1, simple thresholding is applied to the classification of type-(ii) dark lesions. Firstly, screening according to lesion size and shape is executed. Next, lesions with large T-degree are extracted. Lastly, these lesions are classified by using the G-BV-difference and G-ratio. G-ratio is a feature used in the bright lesion classifier, but it is also effective for classifying dark lesions. The threshold for each feature is determined in advance by analyzing the distribution of each feature. The lesion candidate whose features exceed all thresholds is regarded as a true dark lesion in this classification.

Table 1. Characteristics of TLs and FPs

#	size	shape	TLs/FPs tendency
1	small	—	Many TLs.
2	middle	circle	There are many type-(ii) FPs when T-degree is large.
3	large	circle	Almost all FPs.
4	large	line	There are many type-(ii) FPs when T-degree is large.

Table 2. Experimental result

	Sensitivity	Specificity
Conventional system	98%	62%
Proposed system	98%	81%

2.5.3 Experimental results

The proposed system is evaluated by experiments using 85 fundus images with lesions and 223 images without lesions. The images were 700×605 pixels in size and 24-bit RGB color. The experimental results show that the sensitivity of the system is 98% and specificity is 81%. The sensitivity is the ratio of the number of images in which lesions are detected to the number of all images with lesions. The specificity is the ratio of the number of images in which lesions are not detected to the number of images without lesions. The conventional system, which has neither the selection of classifiers nor new features, is also evaluated. The results are listed in Table 2. The new system has improved specificity of 19 points while the sensitivity stays at 98%. This means the new system can remove FPs without decreasing lesion detection rate.

2.5.4 Conclusion

We developed a system to detect fundus lesions of diabetic retinopathy. The system is characterized by a classifier selection controlled by the positions of candidate lesions and a new classifier with several new features to discriminate true lesions and false positive lesions. The proposed techniques can solve the difficulties in classifying the lesions in the area around the blood vessels. Experimental results show the system has improved specificity of 81% and the same sensitivity of 98% as a conventional system. Moreover, the system indicates the position of the lesions by circles as shown in Fig. 8. The white circles indicate the positions of bright lesions, and the black circles indicate the positions of dark lesions.

When analyzing fundus images by batch processing, the system can process about 1,000 images during the night (approximately 12 hours). This throughput is more than the number of images examined in a day at a medical center. We therefore propose that the outputs from the system could be used as a kind of "second opinion" in health examinations.

Our future work includes the automation of building up classifiers by AdaBoost-like techniques.

Acknowledgements The authors wish to thank Prof. Hidefumi Kobatake and Associate Prof. Akinobu Shimizu of Tokyo University of Agriculture and Technology for their comments and advise on medical imaging technologies. Special thanks go to Dr. Tohru Nakagawa of Hitachi Medical Center for providing the information about medical examinations.

References

[1] E. Stefánsson: "Prevention of diabetic blindness", *British Journal of Ophthalmology*, vol. 90, pp. 2-3, Jan. 2006

[2] D. Usher, M. Dumskyj, M. Himaga, T. Williamson, S. Nussey and J. Boyce: "Automated Detection of Diabetic Retinopathy in Digital Retinal Images: a Tool for Diabetic Retinopathy Screening", *Diabetic Medicine*, vol. 21, iss. 1, pp. 84-90, Jan. 2004

[3] D. Usher: "Image Analysis for the Screening of Diabetic Retinopathy", *A thesis of King's College*, University of London

[4] C. Sinthanayothin, J. Boyce, H. Cook and T. Williamson: "Automated localization of the optic disc, fovea, and retinal blood vessels from digital colour fundus images", *British Journal of Ophthalmology*, 83(8), pp. 902-910, Aug. 1999

[5] A. Osareh, M. Mirmehdi, B. Thomas and R. Markham: "Classification and Localisation of Diabetic-Related Eye Disease", *7th European Conference on Computer Vision*, pp. 502-516, May 2002

[6] M. Himaga, D. Usher and J. F. Boyce: "Accurate Retinal Blood Vessel Segmentation by Using Multi-Resolution Matched Filtering and Directional Region Growing", *IEICE Trans. INF. & SYST.*, vol. E87-D, no. 1, pp. 155-163, Jan. 2004

[7] A. D. Hoover, V. Kouznetsova and M. Goldbaum: "Locating blood vessels in retinal images by piecewise threshold probing of a matched filter response", *IEEE Trans. Medical Imaging*, vol. 19, iss. 3, pp. 203-210, Mar. 2000

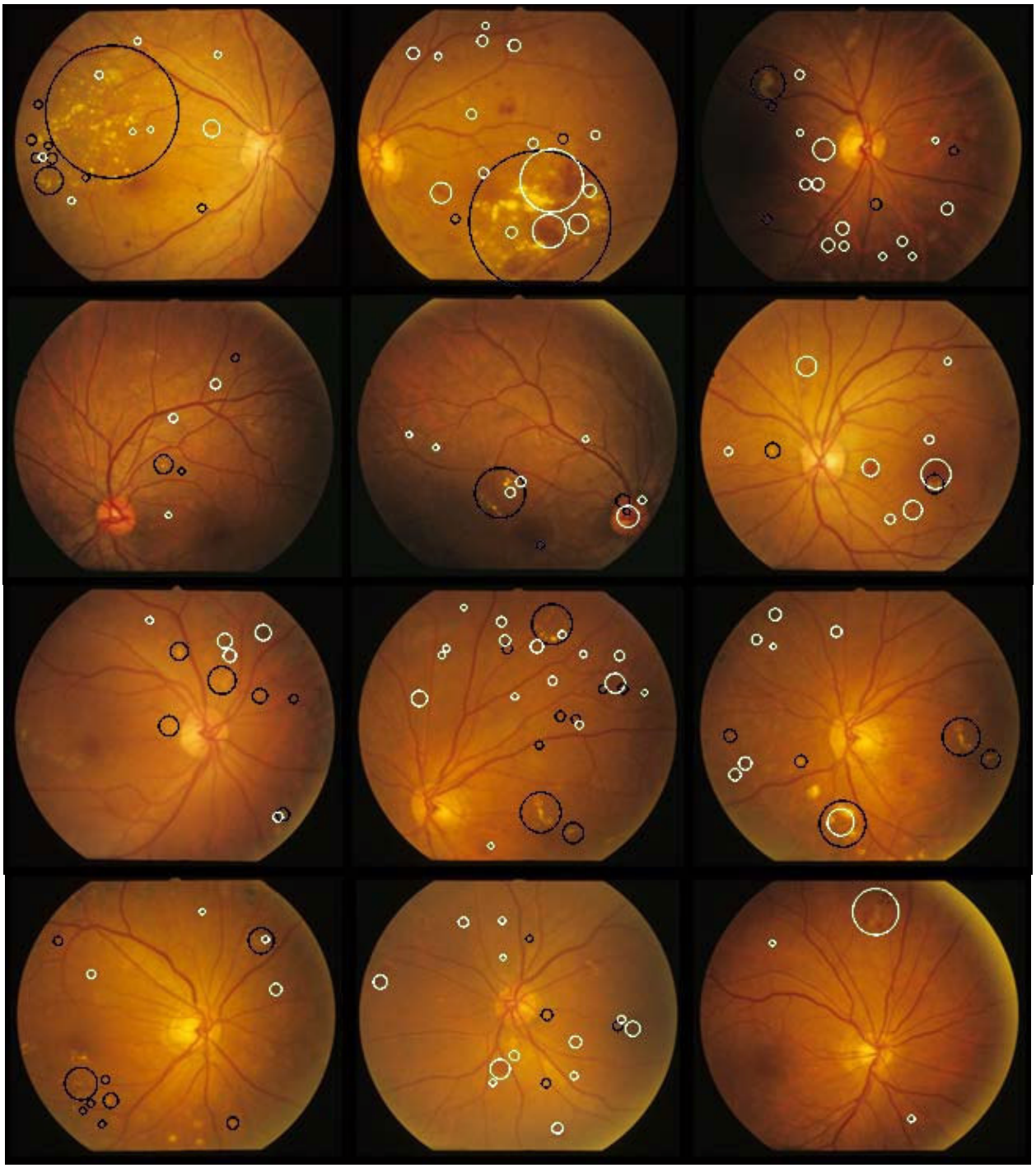

Figure 8: Detected lesions